Organic Electronics 13 (2012) 1038–1043

Contents lists available at SciVerse ScienceDirect

Organic Electronics

journal homepage: www.elsevier.com/locate/orgel

High-efficiency red electroluminescence from europium complex containing a neutral dipyrido(3,2-a:2′,3′-c)phenazine ligand in PLEDs

Yu Liu [a], Yafei Wang [a], Juan He [a], Qingqing Mei [a], Kai Chen [a], Jiaojiao Cui [a], Chun Li [b], Meixiang Zhu [a], Junbiao Peng [b], Weiguo Zhu [a,*], Yong Cao [b,*]

[a] Department of Chemistry, Key Lab of Environment-Friendly Chemistry and Application in the Ministry of Education, Xiangtan University, Xiangtan 411105, PR China
[b] Institute of Polymer Optoelectronic Materials and Devices, South China University of Technology, Guangzhou 510640, PR China

ARTICLE INFO

Article history:
Received 27 November 2011
Received in revised form 10 February 2012
Accepted 25 February 2012
Available online 16 March 2012

Keywords:
Europium(III) complex
Optophysical properties
Electroluminescence
Polymer light-emitting devices

ABSTRACT

In order to obtain high-efficiency monochromatic red emission in polymer light-emitting devices, a tris(dibenzoylmethanato)(dipyrido(3,2-a:2′,3′-c)phenazine) europium [$Eu(DBM)_3$(DPPZ)] doped single-emissive-layer devices were fabricated using a blend of poly(9,9-dioctyl-fluorence) and 2-*tert*-butyl-phenyl-5-biphenyl-1,3,4-oxadiazole as a host matrix by solution process. Significantly improved electro-luminescent properties with sharp red emission at 611.5 nm were displayed in the $Eu(DBM)_3$(DPPZ)-doped devices at dopant concentrations from 1 to 8 wt.%. The highest luminance up to 1783 cd/m^2 at 2 wt.% dopant concentration, as well as the maximum external quantum efficiency of 2.5% and current efficiency of 3.8 cd/A were obtained at 1 wt.% dopant concentration.

1. Introduction

Since the initial work about lanthanide complex was reported by Kido et al. [1], the light-emitting devices used europium(III) complexes as the emitters have been attracting widely interest because they can emit highly monochromatic red light at around 612 nm with half peak bandwidths of 5–10 nm resulting from the $^5D_0 \rightarrow {}^7F_2$ electronic transitions of Eu^{3+} ion, together with a 100% intrinsic quantum efficiency in theory [2]. Among these europium(III) complexes-doped devices, the OLEDs (organic light-emitting devices) fabricated by vacuum deposition have made a great deal of progress in recent decades [3–18]. The maximum external quantum efficiency (*EQE*) of 7.5% at 0.02 mA/cm^2 in the OLEDs with tris(dibenzoylmethanato)-(4,7-biphenyl-1,10-phenanthroline)europium(III) doped into *N*,*N*′-diphenyl-*N*,*N*′-bis(3-methylphenyl)-1,1-biphenyl-4,4-diamine and the highest brightness of 2450 cd/m^2 at 20 V in another OLEDs with tris(dibenzoylmethanato)(3,4,7,8-tetramethyl-1,10-phenanthroline) europium(III) doped into 4-(dicyanomethylene)-2-*tert*-butyl-6-(1,1,7,7-tetramethyljulolid-yl-9-enyl)-4H-pyran were obtained by Kido and Ma groups, respectively [6,9]. However, the reported maximum *EQE* levels were attained only at low current density (~0.01 mA/cm^2). In all case, the *EQE* and brightness of these europium complexes-doped OLEDs were much lower than ones of those iridium complexes-doped OLEDs.

Compared to the europium(III) complexes-doped OLEDs made by vacuum deposition, those europium(III) complexes-doped PLEDs (polymer light-emitting devices) fabricated by spin-coating and printing technique have been developed sluggishly and exhibited much low *EQE* and brightness [19–32]. A highest *EQE* of 4.3% in the PLEDs with 4,4,4,-trifluoro-1-(9,9-dihexylfluoren-2-yl)-1,3-butanedione)(1,10-phen-anthroline)europium(III) doped into a blend of poly(*N*-vinylcarbazole) (PVK) and 2-(*tert*-butylphenyl)-5-biphenyl-1,3,4-oxadiazole (PBD) was reported by Cao group [31]. Recently, we also exhibited a maximum *EQE* of 1.8% and a brightness over 1300 cd/m^2 in the

* Corresponding authors. Tel.: +86 731 58298280; fax: +86 731 58292251 (W. Zhu); tel.: +86 20 87114635 (Y. Cao).
E-mail addresses: zhuwg18@126.com (W. Zhu), yongcao@scut.edu.cn (Y. Cao).

1566-1199/$ - see front matter © 2012 Elsevier B.V. All rights reserved.
http://dx.doi.org/10.1016/j.orgel.2012.02.024

triphenylamine-functionalized ternary europium(III) complex doped PLEDs using a blend of poly(9,9-dioctylfluorene) (PFO) and PBD as the host matrix [32]. It is obvious that the europium(III) complexes-doped PLEDs still remains a significant challenge in *EQE* and brightness.

It is well-known that in rare earth complexes, secondary ligands often play a significant role in tuning optophysical property because of an additional energy transfer from the secondary ligand to the primary ligand or to the central rare earth ions [9]. Compared to the common secondary ligand of phenanthroline (Phen), dipyrido(3,2-a:2′,3′-c)phenazine (DPPZ) has an extended π-conjugation and a larger absorption coefficient. It is expected to make its europium complexes have increasing absorption and improving electroluminescent properties in the devices. Therefore, Sun made tris(4,4,4-trifluoro-1-(2-thienyl)-1,3-butanedionato)(dipyrido(3,2-a:2′,3′-c)phenazine) europium(III)[Eu(TTA)$_3$(DPPZ)] and exhibited a high *EQE* of 2.1% and brightness of 1670 cd/m^2 in the Eu(TTA)$_3$(DPPZ)-doped OLEDs using (4,4′-*N*,*N*′-dicarbazole-bi-phenyl) as host matrix [7].

In this paper, to obtain high-efficiency and high-brightness europium(III) complexes-doped PLEDs, we chose tris(dibenzoylmethanato)(dipyrido(3,2-a:2′,3′-c)phenazine-europium(III) [Eu(DBM)$_3$(DPPZ)] as a dopant to make some double-layer PLEDs using a blend of PFO and PBD as host matrix. As Eu(DBM)$_3$(DPPZ) has red-shifted UV absorption spectrum than Eu(TTA)$_3$(DPPZ), bigger spectral overlap between the absorption profile of europium complex and the emission profile of the PFO–PBD blend is inevitable for Eu(DBM)$_3$(DPPZ). It is suggested that bigger spectral overlap is available to improve device performance for the guest–host-based luminescent devices. For this reason, Eu(DBM)$_3$(DPPZ) is expected to present improved electroluminescent (EL) performance in the made double-layer PLEDs. As expected, highly efficient monochromic red emissions at 611.5 nm with an *EQE* of 2.5% and a brightness of 1445 cd/m^2 were obtained in the Eu(DBM)$_3$(DPPZ)-doped device at 1 wt.% dopant concentration. Furthermore, the maximum brightness is up to 1783 cd/m^2 in the device at 2 wt.% dopant concentration. To the best of our knowledge, these EL efficiency and brightness levels are highest among the reported europium complex-doped PLEDs.

2. Results and discussion

2.1. Physical properties (TGA, DSC and AFM)

The thermal properties of Eu(DBM)$_3$(DPPZ) were studied by thermogravimetric analysis (TGA) and differential scanning calorimetry (DSC) under nitrogen atmosphere, and the TGA and DSC curves are shown in Fig. 1. A high decomposition temperature (T_d) at 300 °C, which corresponds to a 5% weight loss, and a temperature of glass transition (T_g) as high as 328 °C were observed. This T_g level is higher than that of the other reported Eu(III) complexes. It indicates that Eu(DBM)$_3$(DPPZ) with extended rigid structure has an excellent thermal stability property.

To investigate the dispersibility of Eu(DBM)$_3$(DPPZ) in polymer host matrix, the Eu(DBM)$_3$(DPPZ)-doped

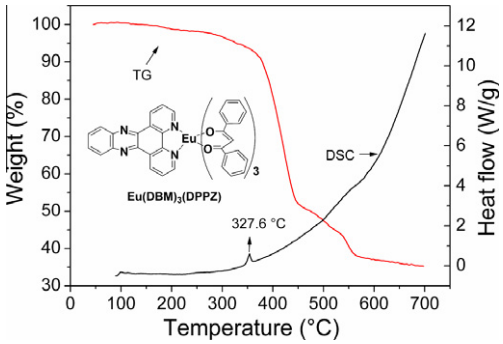

Fig. 1. TG and DSC curves of Eu(DBM)$_3$(DPPZ) recorded in dynamic nitrogen atmosphere (50 mL/min) and at heating rate 10 °C/min for TG and 30 °C/min for DSC test.

PBD–PFO film at 8 wt.% doping concentration was made. The surface morphology was recorded by atomic force microscopy (AFM) and is shown in Fig. 2. A roughness with R_a = 0.739 nm is observed in the Eu(DBM)$_3$(DPPZ) doped film. It indicates that Eu(DBM)$_3$(DPPZ) has a good dispersibility in the PFO–PBD host matrix [32]. In general, the extended π-conjugated system is available to enhance the intermolecular π–π effect between the dopant and host matrix, further facilitate the dopant to disperse in the host matrix. As a result, the good dispersibility is considered to be related to the extended π-conjugation of DPPZ.

2.2. Optical analysis

The normalized UV–vis absorption spectrum of Eu(DBM)$_3$(DPPZ) in thin film, and the photoluminescence (PL) spectrum of the PFO–PBD (30 wt.%) blend film are shown in Fig. 3. Two typical UV–vis absorption peaks at 260 and 361 nm are observed, where the former is attributed to the DPPZ ligand-centered π–π* electron transition and the latter is assigned to the DBM ligand-centered π–π* electron transition. Compared to the low-lying absorption peak (at 340 nm) of Eu(TTA)$_3$(DPPZ) [7], this Eu(DBM)$_3$(DPPZ) exhibited a red-shifted UV–vis absorption profile. Consequently, a bigger spectral overlap between the emission spectrum of the PFO–PBD blend film and the absorption spectrum of Eu(DBM)$_3$(DPPZ) rather than Eu(TTA)$_3$(DPPZ) is displayed. It is suggested that the enhanced spectral overlap are useful for Förster energy transfer from the host to the europium complex [20,31].

Fig. 3 also shows the PL spectrum of Eu(DBM)$_3$(DPPZ) in dichloromethane (DCM). An intense sharp emission peak at 612 nm with a full width at half maximum (FWHM) of 8 nm is observed under 346 nm photo-excitation, which corresponds to the $^5D_0 \rightarrow {}^7F_2$ transition of Eu^{3+} ion. No emission from the DPPZ ligand was exhibited. This means that an efficient energy transfer occurs from DPPZ to Eu^{3+} ion [6]. To further understand the influence of the secondary ligand on PL of its europium complex, the PL quantum yield (Φ_{PL}) of Eu(DBM)$_3$(DPPZ) was measured in degassed DCM by using $EuCl_3{\cdot}6H_2O$ (Φ_f = 0.73% in water) as the standard at ambient temperature [33]. A Φ_{PL} of 27.1% was obtained in the degassed DCM solution of Eu(DBM)$_3$(DPPZ). This level is bout 35 times higher than that of

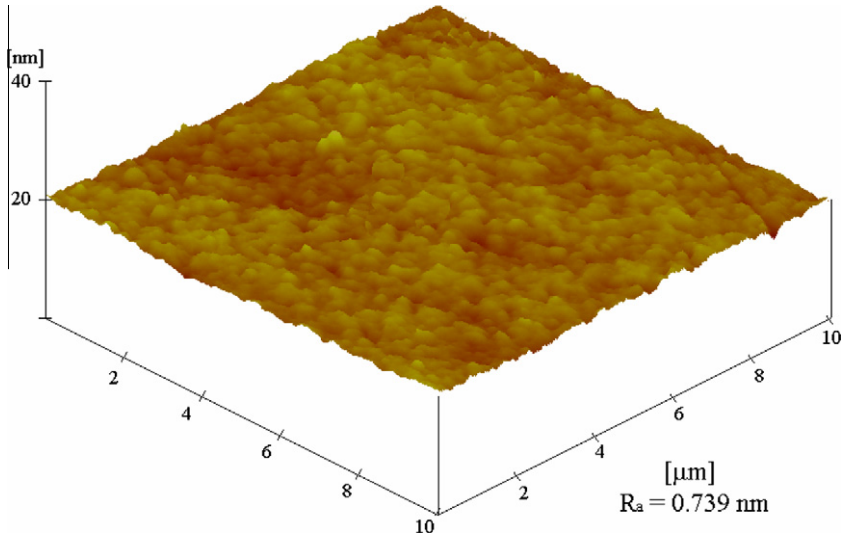

Fig. 2. Atomic force microscope images of the $Eu(DBM)_3(DPPz)$-doped PFO–PBD film at 8 wt.% dopant concentration. The scanning range is 10 μm by 10 μm, and the film thickness was about 80 nm.

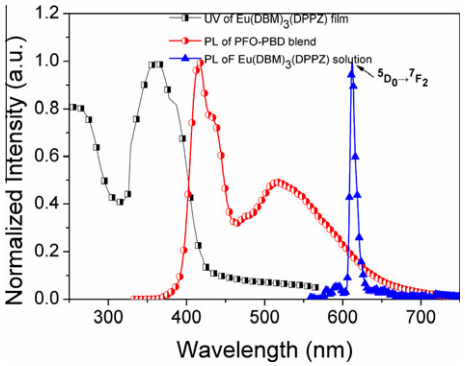

Fig. 3. The normalized UV–vis absorption spectra of $Eu(DBM)_3(DPPZ)$ in thin film, and the normalized PL spectrum of the PFO–PBD (30 wt.%) blend film and $Eu(DBM)_3(DPPZ)$ in DCM (λ_{ex} = 346 nm), respectively.

$Eu(DBM)_3(Phen)$ [32]. The improved Φ_{PL} may be related to complex symmetry and more efficient sensitization of Eu^{3+} ion by the secondary ligand of DPPZ. While the large rigid DPPZ ligand was introduced into europium complex, its site isolation effect is evident for its europium complex in DCM solution, which is available for the antenna effect from the ligand to the center Eu^{3+} ion. Therefore, the Φ_{PL} of $Eu(DBM)_3(DPPZ)$ was effectively improved [34].

To investigate Förster energy transfer under solid state, the $Eu(DBM)_3(DPPZ)$-doped PFO–PBD (30 wt.%) films at various dopant concentrations from 1 to 8 wt.% were made. Fig. 4a shows the normalized PL spectra of these $Eu(DBM)_3(DPPZ)$-doped PFO–PBD (30 wt.%) films under excitation of He–Cd laser (325 nm). Two intense emission peaks at about 416 and 515 nm are observed in all of these doped films, which are similar to those of the PFO–PBD blend film. In additional, a serious of weak emission peaks at about 592, 612 and 652 nm, coming from Eu^{3+} emission are also observed at the given dopant concentrations. Furthermore, the emission intensity at 612 nm increases

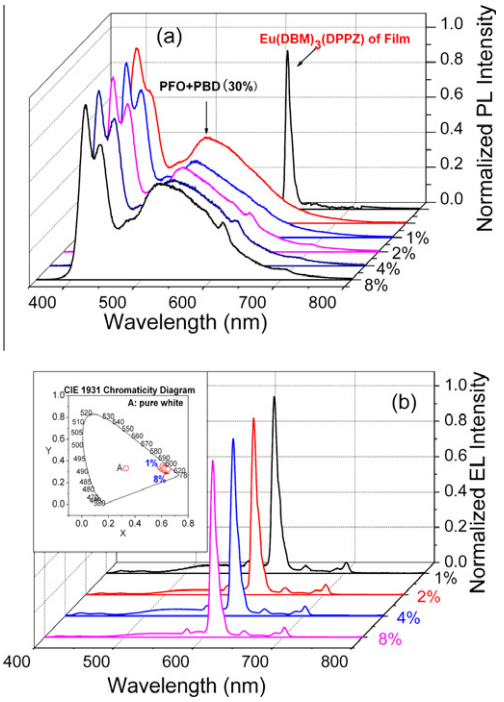

Fig. 4. (a) The normalized PL spectra of the $Eu(DBM)_3(DPPZ)$-doped PFO–PBD (30 wt.%) films at different concentrations from 1 to 8 wt.%, respectively. (b) The normalized EL spectra of the $Eu(DBM)_3(DPPZ)$-doped PFO–PBD (30 wt.%) devices at different concentrations from 1 to 8 wt.%, respectively. CIE 1931 chromaticity diagrams of these corresponding devices.

gradually with increasing dopant concentrations from 1 to 8 wt.%. This indicates that PL processes of the $Eu(DBM)_3(DPPZ)$-doped PFO–PBD films are dominated by the PFO–PBD blend. As the spectral overlap between PFO–PBD emission and $Eu(DBM)_3(DPPZ)$ absorption is

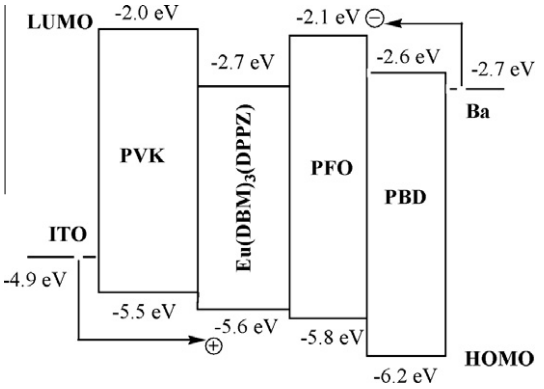

Fig. 5. The energy levels diagram of the PLED used in this study.

small and the theoretical Förster radius (R_0) is only 1.5 nm in the blending system between PFO and europium complex [23], the inefficient Förster resonance energy transfer (FRET) from the PFO–PBD to the central Eu^{3+} ion is bound to occur in the $Eu(DBM)_3(DPPZ)$-doped PFO–PBD films under photo-excitation [21,23–27].

It is noted that the absolute PL quantum efficiencies of the $Eu(DBM)_3(DPPZ)$-doped films gradually decrease with increasing dopant concentrations. The measured PL quantum efficiencies were 39.10%, 32.87%, 31.47% and 31.28% for these doped films at doping concentrations of 1, 2, 4, and 8 wt.%, respectively. Here, the host matrix PL is somewhat quenched but the Eu-complex emission is enhanced in this doped system by increasing the doping concentration. This similar phenomenon was also observed by Giovanella and Rothe groups, which is related to singlet energy transfer from PFO to Eu-complex and triplet energy transfer from the ligand of Eu-complex back to PFO [23,35]. As the Dexter-type energy transfer process from the ligand of europium complex to the host PFO triplets (backflow of excitation or back-transfer) is competitive with the singlet energy transfer process, the emission efficiency of the system was strongly reduced in this doped system.

2.3. Electrochemistry property

In order to understand why $Eu(DBM)_3(DPPZ)$ presented high efficiency and luminance in the devices, the electrochemical property of $Eu(DBM)_3(DPPZ)$ was examined by cyclic voltammetry (CV). Its reversible oxidation wave (E_{ox}) and reduction wave (E_{red}) were measured to 0.86 V and −2.04 V, respectively. According to an empirical formula [36,37], the lowest unoccupied molecular orbital (LUMO) and the highest occupied molecular orbital (HOMO) energy levels for $Eu(DBM)_3(DPPZ)$ were calculated to be −2.70 and −5.60 eV, respectively. Fig. 5 shows the energy level diagram of the devices. The HOMO and LUMO energy levels for the other used materials were obtained from the previous reports [38,39]. Since the HOMO and LUMO energy levels of PFO respectively are −5.8 and −2.1 eV, it indicates that $Eu(DBM)_3(DPPZ)$ as dopant can more efficiently trap carriers with respect to PFO.

2.4. Electroluminescent properties

The normalized EL spectra of the $Eu(DBM)_3(DPPZ)$-doped PFO–PBD devices at different dopant concentrations from 1 to 8 wt.% are shown in Fig. 4b. A significantly sharp EL emission peak at 611.5 nm with a FWHM of 10 nm is observed at the different dopant concentrations, which generates from the $^5D_0 \rightarrow {}^7F_2$ electronic transition. At the same time, three weak emission peaks were also exhibited, which is assigned to the $^5D_0 \rightarrow {}^7F_0$ (579 nm), $^5D_0 \rightarrow {}^7F_3$ (651 nm) and $^5D_0 \rightarrow {}^7F_4$ (702 nm) transitions of Eu^{3+} ion, respectively. In additional, a minor high-lying emission peak at 515 nm from the PFO–PBD blend was appeared and reduced with increasing dopant concentrations. The corresponding CIE chromaticity coordinates (X, Y) varied from (0.607, 0.349) to (0.647, 0.331) (Table 1) with increasing dopant concentrations from 1 to 8 wt.%. Hence, the EL spectra in these devices are dominated by $Eu(DBM)_3(DPPZ)$ and have changed very little. The substantial difference between PL spectra of the doped films and EL spectra is suggested to be attributed to charge-trapping effect on $Eu(DBM)_3(DPPZ)$ and is further supported by above electro-chemical properties of $Eu(DBM)_3(DPPZ)$ [25,26,30–32].

Fig. 6 shows the current densities (J)–voltage (V)–brightness (B) characteristics of the europium complex-doped PFO–PBD devices, and the electroluminescence data are summarized in Table 1. A maximum brightness of 1783 cd/m^2 at 183.2 mA/cm^2 was obtained in the device at 2 wt.% doping concentration. Even at the 100 mA/cm^2, the device remained brightness as high as 1445 cd/m^2. On the other hand, the turn-on voltage of the devices

Table 1
Device performances of the $Eu(DBM)_3(DPPZ)$-doped PFO–PBD (30 wt.%) devices at different dopant concentrations from 1 to 8 wt.%.

Dopant ratio[a] (wt.%)	Turn-on voltage (V)	Maximum *EQE*[b]			*J* = 100 mA/cm^2		Maximum *B*		CIE (*X*, *Y*)
		J (mA/cm^2)	*EQE* (%)	*LE*[c] (cd/A)	*L*[c] (cd/m2)	*EQE* (%)	*L* (cd/m^2)	*J* (mA/cm^2)	
1	7.3	2.5	2.5	3.8	1381	0.90	1445	124.4	0.607, 0349
2	10.4	4.4	1.8	3.6	1445	0.96	1783	183.2	0.617, 0.335
4	13.6	1.7	1.6	2.4	1058	0.70	1137	120.7	0.628, 0.338
8	16.1	1.3	1.5	2.3	451[b]	0.57[b]	606	84.9	0.649, 0.321

[a] The doping concentrations of $Eu(DBM)_3(DPPZ)$ in the device with a configuration of ITO/PEDOT:PSS, 50 nm/PVK, 40 nm/$Eu(DBM)_3(DPPZ)$ + PFO–PBD, 80 nm/Ba, 4 nm/Al, 150 nm.

[b] At the current density of 50 mA/cm^2.

[c] The luminance (L) and luminous efficiency (LE) were measured with a silicon photodiode and calibrated using a PR-705 SpectraScan Spectrophotometer (Photo Research).

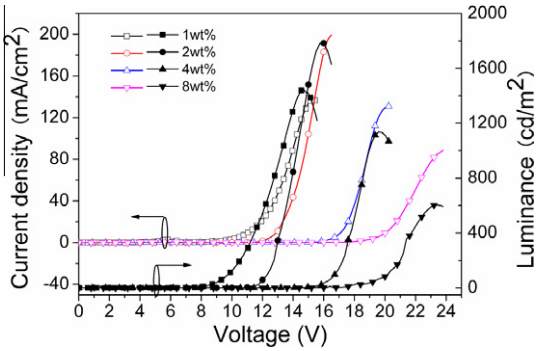

Fig. 6. The current density–voltage–brightness (*J–V–B*) characteristics of the $Eu(DBM)_3(DPPZ)$-doped PFO–PBD (30 wt.%) devices at different dopant concentrations from 1 to 8 wt.%, respectively.

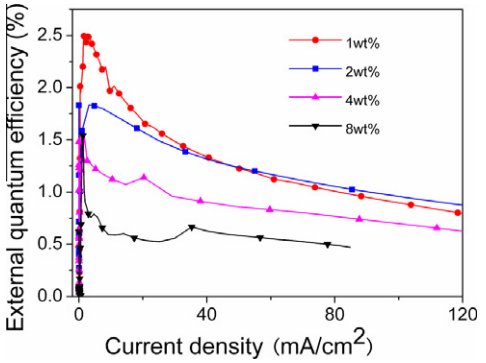

Fig. 7. The external quantum efficiency–current density characteristic of the $Eu(DBM)_3(DPPZ)$-doped PFO–PBD (30 wt.%) devices at different dopant concentrations from 1 to 8 wt.%, respectively.

increases from 7.2 to 16.1 V with increasing doping level from 1 to 8 wt.%. This also indicates that the devices are mainly operated by the carrier-trapping mechanism based on the identical phenomenon observed previously by Chang et al. [39]. To the best of our knowledge, this is one of the best EL properties in the PLEDs used europium complex as a single dopant [19–32].

Fig. 7 shows the external quantum efficiency–current density characteristics of the $Eu(DBM)_3(DPPZ)$-doped PFO–PBD devices at different doping concentrations. The device with 1 wt.% doping concentration demonstrated the best device performance. The maximum luminous efficiency of 3.8 cd/A and external quantum efficiency of 2.5% at current density of 2.5 mA/cm^2 are exhibited, respectively. Even at the dopant concentration of 8 wt.%, the device still maintained a maximum *EQE* as high as 1.5%. This phenomenon indicates that the concentration quenching of the $Eu(DBM)_3(DPPZ)$ dopant was efficiently suppressed at high dopant concentrations compared to our previous work [26,32]. Distinctly, increasing the rigid structure of the neutral ligand is available to improve the devices performance and suppress the emission quenching for europium complexes.

3. Conclusions

In summary, we investigated the photophysical and electrochemical properties of $Eu(DBM)_3(DPPZ)$, further the electroluminescent properties of its double-layer doped PFO–PBD PLEDs. The maximum luminance of 1783 cd/m^2 at 183.2 mA/cm^2, as well as the maximum *EQE* of 2.5% and luminous efficiency of 3.8 cd/A were obtained in the devices using $Eu(DBM)_3(DPPZ)$ as dopant. Our results demonstrate that it is possible to achieve high-efficiency sharp red emission of europium complex in the PLEDs by extending rigid conjugation secondary ligand.

4. Experimental section

4.1. Materials

The europium complex of $Eu(DBM)_3(DPPZ)$ was synthesized following the literature method and its molecular structure is shown in Fig. 1(inset) [23]. The complex of $Eu(DBM)_3(DPPZ)$ was characterized by elemental analysis.

4.2. Methods

Elemental analyses (C, H, N) were performed with a Perkin-Elmer 240 instrument. Thermogravimetric analyze (TGA) was carried out with a NETZSCH STA 449 in nitrogen atmosphere at a heating rate of 10 °C/min from 10 to 700 °C. Differential scanning calorimetry (DSC) was carried out with a NETZSCH DSC 204 at a heating rate of 30 °C/min from 25 to 700 °C under nitrogen atmosphere. UV–vis spectra were recorded with a HP-8453 system. Photoluminescence (PL) spectra were recorded under excitation of a He:Cd laser at 325 nm. Cyclic voltammetry experiments were performed using a CHI660A electro-chemical work station at room temperature. A conventional three-electrode configuration consisting of a glassy carbon working electrode, a platinum wire auxiliary electrode, and an anhydrous Hg/Hg_2Cl_2 reference electrode was used. The supporting electrolyte was tetrabutyl ammonium hexafluorophosphate (Bu_4N-PF_6) (0.1 M) in acetonitrile. Ferrocene was added as a calibration after each set of measurements and all reported potentials were quoted with reference to the ferrocene/ferrocenium (Fc/Fc^+) couple at a scan rate of 50 mV/s. As a result, the highest occupied molecular orbit (HOMO) and the lowest unoccupied molecular orbit (LUMO) energy levels of this complex, E_{HOMO} and E_{LUMO} are calculated according to the following equation, $E_{LUMO} = -(E_{red} + 4.74)$ eV and $E_{HOMO} = -(E_{oxd} + 4.74)$ eV, where −4.74 eV is energy level of the SCE with respect to the zero vacuum level [36,37].

4.3. Device fabrication and characterization

PLEDs were fabricated on a cleaned indium-tin oxide (ITO) glass substrate with a sheet resistance of 15 Ω/sq and a thickness of 120 nm in a controlled N_2-filled dry box (Vacuum Atmosphere Co.) under N_2 circulation with oxygen and water contents less than 1 ppm, which had a configuration of ITO/PEDOT:PSS, 50 nm/PVK, 40 nm/$Eu(DBM)_3$

(DPPZ) + PFO–PBD, 80 nm/Ba, 4 nm/Al, 150 nm. In the made process, a 50 nm hole-injection layer of poly(3,4-ethylenedioxy-thiophene):poly(styrenesulfonic acid) (PEDOT:PSS, Batron-P4083, purchased from Bayer AG) was firstly spin-coated onto a precleaned ITO surface and then baked at 80 °C for 12 h under vacuum to improve hole injection and to increase substrate smoothness. Secondary, a 40 nm poly(*N*-vinylcarbazole) (PVK, $M_w = 1 \times 10^6$ g/mol) was used as hole-transporting layer was spin-coated onto the PEDOT:PSS layer from chlorobenzene solution, and annealed for 2 h at 80 °C. To prevent dissolving the hole-transporting PVK layer, the emitting layer containing PFO ($M_w = 5.8 \times 10^4$ g/mol)/PBD/europium complex was spin-coated onto the PVK layer from toluene solution, in which PVK is nearly insoluble, thus the two layers may stay relatively separated. The doping concentrations of europium complex in emitting layer were 1, 2, 4 and 8 wt.%, respectively. The spin-coated thickness was measured with an Alpha-step 500 surface profiler (Tencor, Alfa-Step 500). Finally, 4 nm barium layer used as the cathode and 150 nm aluminum used as capping layer were successively deposited on the top of emitting layer through a shadow mask in vacuum (3×10^{-4} Pa). The deposition speed and thickness of barium and aluminum layers were monitored with a thickness/rate meter Model STM-100 (Sycon Instrument, Inc.).

Current density (*J*)–voltage (V) data were collected using a Keithley 236 source meter. Absolute PL efficiencies for the doped films were measured in the integrating sphere (IS-080, Labsphere) under the 325 nm line of a He–Cd laser. The luminance (cd m^{-2}) was measured by using a Si photodiode. *EQE* were obtained by measuring the total light output in all directions in an integrating sphere (IS-080, Labsphere). PL and EL spectra were recorded by using a charge-coupled device (CCD) spectrophotometer (Instaspec 4, Oriel) and CIE coordinates were recorded using PR-705 SpectraScan spectrophotometer (Photo Research).

Acknowledgments

The authors thank the National Natural Science Foundation of China (Project Nos. 20872124, 20772101 and 50973053), the Specialized Research Fund and New Teacher Fund for the Doctoral Program of Higher Education (20094301110004, 200805301013), the Open Project Program of Key Laboratory of Environmentally Friendly Chemistry and Applications of Ministry of Education (09HJYH06), the Scientific Research Fund of Hunan Provincial Education Department (11CY023, 10A119, 10B112), the Hunan Provincial Natural Science Foundation of China (11JJ3061), the Postgraduate Science Foundation for Innovation in Hunan Province (CX2011263) and Hunan Undergraduate Investigated-Study and Innovated-Experiment Plan for the financial support of this research.

References

[1] J. Kido, K. Nagai, Y. Ohashi, Chem. Lett. (1990) 657.
[2] A. Edwards, C. Claude, I. Sokolik, T.Y. Chu, Y. Okamoto, R. Dorsinvill, J. Appl. Phys. 82 (1997) 1841.
[3] Z. Hong, C.J. Liang, R.G. Li, W.L. Li, D. Zha, D. Fan, D.Y. Wang, B. Chu, F.X. Zang, L.S. Hong, S.T. Lee, Adv. Mater. 13 (2001) 1241.
[4] P.P. Sun, J.P. Duan, H.T. Shih, C.H. Cheng, Appl. Phys. Lett. 81 (2002) 792.
[5] M. Sun, H. Xin, K.Z. Wang, A.Y. Zhang, L.P. Jin, C.H. Huang, Chem. Commun. (2003) 702.
[6] C.T.W. Canzler, J. Kido, Org. Electron. 7 (2006) 29.
[7] P.P. Sun, J.P. Duan, J.J. Lih, C.H. Cheng, Adv. Funct. Mater. 13 (2003) 683.
[8] Z.R. Hong, C.S. Lee, S.T. Lee, W.L. Li, S.Y. Liu, Appl. Phys. Lett. 82 (2003) 2218.
[9] J.F. Fang, H. You, J. Gao, D.G. Ma, Chem. Phys. Lett. 392 (2004) 11.
[10] M. Guan, Z.Q. Bian, F.Y. Li, H. Xin, C.H. Wang, New J. Chem. 27 (2003) 1731.
[11] T. Oyamada, Y. Kawamura, T. Koyama, N. Sasabe, C. Adachi, Adv. Mater. 16 (2004) 1082.
[12] Q. Jin, W.L. Li, G.B. Che, W.M. Su, X.Y. Sun, B. Chu, B. Li, Appl. Phys. Lett. 89 (2006) 223524.
[13] C.J. Liang, D. Zhao, Z.R. Hong, D.X. Zhao, X.Y. Liu, W.L. Li, Appl. Phys. Lett. 76 (2006) 67.
[14] L. Zhou, H.J. Zhang, W.D. Shi, R.P. Deng, Z.F. Li, J.B. Yu, Z.Y. Guo, J. Appl. Phys. 104 (2008) 114507.
[15] H. Xu, K. Yin, W. Huang, Chem. Phys. Chem. 9 (2008) 1752.
[16] H.J. Tang, H. Tang, Z.G. Zhang, J.B. Yuana, C.J. Cong, K.L. Zhang, Synth. Met. 159 (2009) 72.
[17] Y.H. Zhou, L. Zhou, J. Wu, H.Y. Li, Y.X. Zheng, X.Z. You, H.J. Zhang, Thin Solid Films 518 (2010) 4403.
[18] H. Xu, K. Yin, W. Huang, J. Phys. Chem. C 114 (2010) 1674.
[19] B. Peng, N. Takada, N. Minami, Thin Solid Films 405 (2002) 224.
[20] J.F. Fang, C.C. Choy, D.G. Ma, E.C.W. Ou, Thin Solid Films 515 (2006) 2419.
[21] M.D. McGehee, T. Bergstedt, C. Zhang, A.P. Saab, M.B. O'Regan, G.C. Bazan, A.I. Srdanov, A.J. Heeger, Adv. Mater. 11 (1999) 1349.
[22] F. Zhang, Z. Xu, S. Zhao, L. Wang, L. Lu, Solid-State Electron. 52 (2008) 1806.
[23] U. Giovanella, M. Pasini, C. Freund, C. Botta, W. Porzio, S. Destri, J. Phys. Chem. C 113 (2009) 2290.
[24] M.A.D. García, S.F.D. Ávila, M.G. Kuzyk, Appl. Phys. Lett. 81 (2002) 3924.
[25] X. Gong, J.C. Ostrowski, D. Moses, G.C. Bazan, A.J. Heeger, Adv. Funct. Mater. 13 (2003) 439.
[26] Y. Liu, J.D. Li, C. Li, J.G. Song, Y.L. Zhang, J.B. Peng, X.Y. Wang, M.X. Zhu, Y. Cao, W.G. Zhu, Chem. Phys. Lett. 433 (2007) 331.
[27] M.R. Robinson, J.C. Ostrowski, G.C. Bazan, M.D. McGehee, Adv. Mater. 15 (2003) 1547.
[28] X. Jiang, A.K.Y. Jen, G.D. Phelan, D. Huang, T.M. Londergan, L.R. Dalton, R.A. Register, Thin Solid Films 416 (2002) 212.
[29] A. O'Riordan, E. O'Connor, S. Moynihan, X. Llinares, R.V. Deun, P. Fias, P. Nockemann, K. Binnemans, G. Redmond, Thin Solid Films 491 (2005) 264.
[30] Z.J. Wang, I.D.W. Samuel, J. Lumin. 111 (2005) 199.
[31] Y. Zhang, C. Li, H. Shi, B. Du, W. Yang, Y. Cao, New J. Chem. 31 (2007) 569.
[32] Y. Liu, Y.F. Wang, H.P. Guo, M.X. Zhu, C. Li, J.B. Peng, W.G. Zhu, Y. Cao, J. Phys. Chem. C 115 (2011) 4209.
[33] Z.Q. Bian, D.Q. Gao, M. Guang, H. Xin, F.Y. Li, K.Z. Wang, L.P. Jin, C.H. Wang, Sci. China B: Chem. 34 (2004) 113 (in Chinese).
[34] Y. Zhang, H.H. Shi, Y. Ke, Y. Cao, J. Lumin. 124 (2007) 51.
[35] C. Rothe, L.O. Palsson, A.P. Monkman, Chem. Phys. 285 (2002) 95.
[36] Z.Y. Hu, C.P. Luo, L. Wang, F.L. Huang, K.M. Zhu, Y.F. Wang, M.X. Zhu, W.G. Zhu, Y. Cao, Chem. Phys. Lett. 441 (2007) 277.
[37] Z.J. Si, J. Li, B. Li, Z.R. Hong, S.Y. Liu, W.L. Li, J. Phys. Chem. C 112 (2008) 3920.
[38] X. Gong, D. Moss, A.J. Heeger, S. Liu, A.K.Y. Jen, Appl. Phys. Lett. 83 (2003) 183.
[39] S.Y. Chang, J. Kavitha, S.W. Li, C.S. Hsu, Y. Chi, Inorg. Chem. 45 (2006) 137.